Insights into 5, 5'-bis(1H-tetrazol-5-yl) amine (BTA) pyrolysis mechanism: Integrated experimental and kinetic model analysis

Jianwei Zhang[a,b], Ling Chen[a,b*], Peichen Han[a,b], Chunzhi Li[d], Ye Yuan[d], Bo Wu[c], Feiyun Chen[a,b], Weidong He[a,b*]

[a] School of Chemistry and Chemical Engineering, Nanjing University of Science and Technology, Nanjing, Jiangsu, 210094, China;

[b] Key Laboratory of Special Energy Materials, Ministry of Education, Nanjing, Jiangsu, 210094, China;

[c] State Key Laboratory of Environment-friendly Energy Materials, Southwest University of Science and Technology, Mianyang, 621010, China;

[d] Scientific Research Institute, Luzhou North Chemistry Industry Corporation, Luzhou, Sicuan, 646605, China;

Corresponding Email:

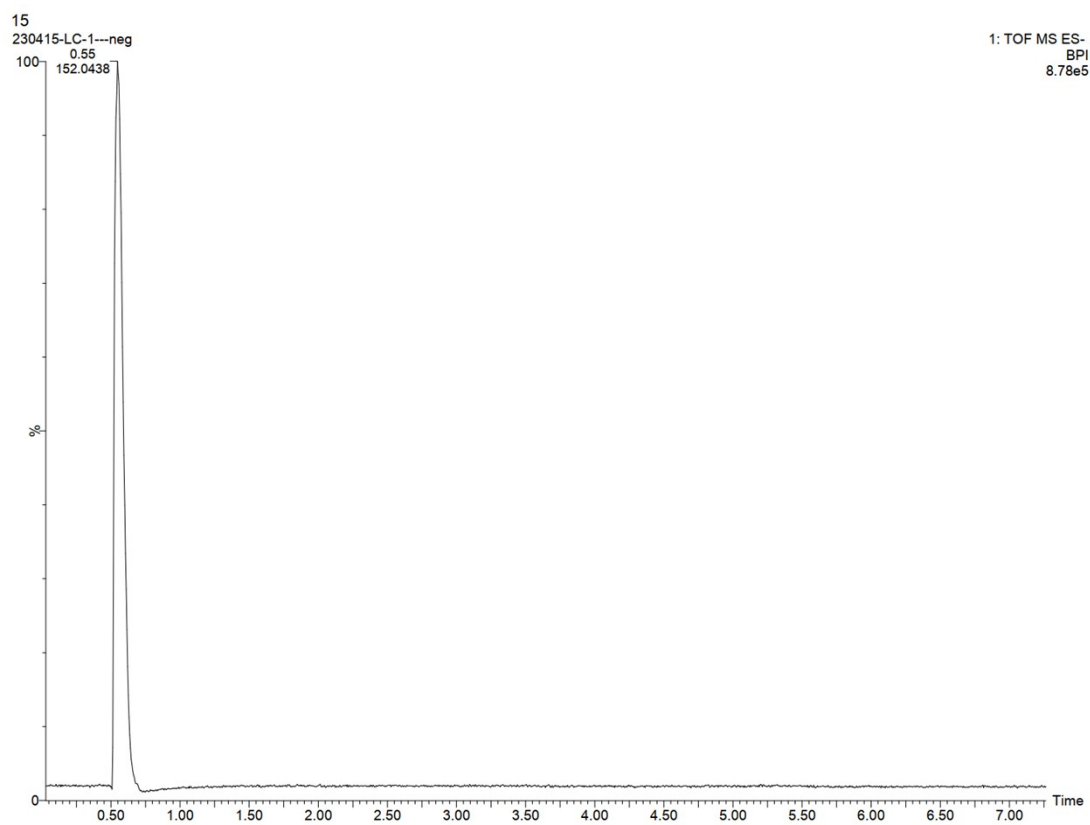Ling Chen: l_chen_zf_139@njust.edu.cn; Weidong He: hewedong@njust.edu.cn;

S1. Materials

Fig S1. HPLC curves of BTA•H$_2$O under alkaline condition.

S2. Thermal analysis methods

TG-DTG measurements were performed in the temperature range 50 °C to 800 °C at the heating rate of 1, 2, 5, 10 °C•min^{-1}, under argon atmosphere at a flow rate of 20 mL•min^{-1} by using PerkinElmer STA 8000. The sample mass was adbot 0.60 mg. A blank test was performed prior to each experiment to obtain a baseline to eliminate systematic errors in this instrument.

DSC measurements of samples were run by NETZSCH DSC 204F1. Alumina crucibles with a lid having small (pin size) hole in the center were used. The scavenging gas and protective gas were nitrogen and the flow rate was 40 mL•min^{-1} and 60 mL•min^{-1}, respectively. The sample mass was about 0.60 mg. The sample was tested at the heating rate of 2 °C•min^{-1} within the temperature range of 50 °C to 300 °C.

S3. Morphology, structure and composition analysis

TableS1. Crystallographic data and parameters.

	BTA•H$_2$O	BTA
Formula	C$_2$H$_5$N$_9$O	C$_2$H$_3$N$_9$
Crystal system	Monoclinic	Orthorhombic
Space group	$P2_1/c$ (14)	$Pbca$ (61)
Color/habit	Colorless/plates	Colorless/needles
ρ/(g cm^{-3})	1.693	1.861
CCDC	687771	299051

TableS2. The high resolution N1s spectra analysis results of BTA•H$_2$O and BTA.

Species	BTA-H$_2$O		BTA	
	Peak/eV	Content	Peak/eV	Content
N1 (C=N̲-N)	399.5	13.6	399.4	12.7
N2 (N=N̲-N)	400.1	20.1	400.0	17.3
N3 (C-N̲(H)-C)	400.8	24.2	400.7	25.8
N4(C-N̲(H)-N)	401.3	27.4	401.2	28.3
N5 (=N$^+$H$^-$)	401.9	14.6	401.8	15.9

S4. TG-DTG and DSC curves analysis
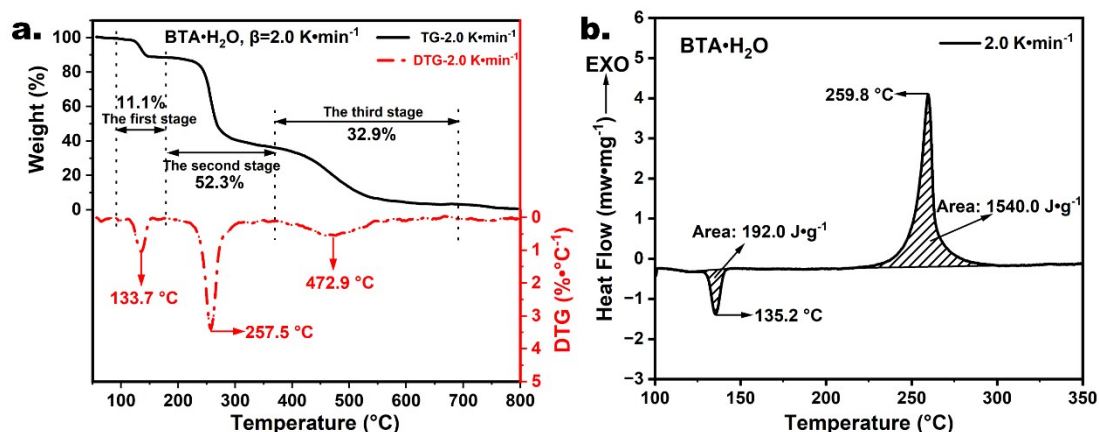

Fig.S2. The TG-DTG (a.) and DSC (b.) curves of BTA•H_2O at the heating rate of 2 K•min^{-1}.

The TG and DTG curves for BTA•H_2O pyrolysis at a heating rate of 2 °C•min^{-1} were presented in **Fig.S2a**, illustrating the typical thermal behavior. Based on the shape of the TG-DTG curve, it was evident that thermal decomposition process of BTA•H_2O involved a complex reaction with three primary mass loss processes. The initial mass loss process (91.1 °C ~178.5 °C) corresponded to the removal of crystalline water within the molecule, resulting in a weight loss of 11.1% and a DTG peak temperature at 133.7 °C. The second mass loss process (178.5 °C ~ 368.4 °C) exhibited a distinct weight reduction of 52.3% and a DTG peak temperature at 257.5 °C, indicating the conversion of a portion of BTA into gaseous compounds containing carbon and nitrogen elements. Subsequently, there was a gradual decrease in weight starting from 368.4 °C until complete decomposition occurred with almost no residue remaining as the temperature reached 690.5 °C. Notably, chemical reactions among residual components primarily contributed to a mass loss of 32.9%, with the maximum weight reduction observed at 472.9 °C.

According to the DSC curve obtained at a heating rate of 2 °C•min^{-1}, as depicted in **Fig.S2b**, two distinct processes were observed. The first process was an endothermic reaction attributed to the loss of crystalline water, characterized by a decomposition peak temperature of 135.2 °C and an

enthalpy change of -192.0 J•g^{-1}. The second process corresponded to the thermal decomposition of BTA and exhibited significant exothermic behavior within the temperature range of 213.4 °C to 301.1 °C, with a decomposition peak temperature recorded at 259.8 °C and an enthalpy change measured at 1540.0 J•g^{-1}. Notably, the sharp exothermic peak indicated that the thermal decomposition process of BTA occurred rapidly, consistent with instantaneous energy release from energetic materials.

S5. Pyrolysis process and product analysis

TableS3. Detailed information of C 1s, N1s and O1s spectra from BTA and pyrolysis products of BTA at 212.5 °C form XPS analysis, indicating peak position, FWHM and Area.

Species	BTA			BTA-212.5 °C		
	Peak/eV	FWHM	Area	Peak/eV	FWHM	Area
Adc	284.80	1.41	5146.48	285.10	1.43	7513.76
C1	286.50	1.87	2980.40	287.18	1.81	2158.73
C2(N-C(-N)-N)	288.40	1.38	23039.62	288.69	1.35	27592.73
N1 (C=N-N)	399.61	1.02	19717.81	399.73	1.10	23453.86
N2 (N=N-N)	400.24	0.85	26794.99	400.4	0.90	34610.45
N3 (C-N(H)-C)	400.87	0.78	39900.61	401.05	0.79	49039.89
N4 (C-N(H)-N)	401.43	0.84	43786.03	401.61	0.79	53771.79
N5 (Positive N)	401.80	1.05	24539.12	401.61	0.96	29196.53
O2	532.75	2.19	6059.21	532.97	2.56	5240.02

TableS4. Detailed information of C 1s, N1s and O1s spectra from pyrolysis products of BTA at 225.0 °C and 237.5 °C form XPS analysis, indicating peak position, FWHM and Area.

Species	BTA-225.0 °C			BTA-237.5 °C		
	Peak/eV	FWHM	Area	Peak/eV	FWHM	Area
Adc	285.13	1.38	4338.72	284.94	1.33	7385.06
C1	286.91	1.54	1669.33	286.80	1.67	3063.25
C2(N-C(-N)-N)	288.76	1.33	15560.65	288.65	1.37	26043.12
C3(Csp²-N)	287.89	1.25	3272.20	287.83	1.27	7833.36
N1 (C=N-N)	400.05	0.90	21457.52	399.84	0.82	34165.87
N2 (N=N-N)	400.67	0.77	24850.35	400.45	0.74	38455.79
N3 (C-N(H)-C)	401.22	0.72	27691.86	401.02	0.71	43534.02
N4 (C-N(H)-N)	401.73	0.78	29387.03	401.55	0.76	42950.80
N5 (Positive N)	402.31	0.95	14428.75	402.15	0.90	21003.69
N6	399.38	1.11	10414.18	399.16	0.99	18281.93
O1	-	-	-	531.65	1.26	2626.05
O2	532.91	2.44	4131.60	532.49	1.21	2417.25
O3	-	-	-	533.47	1.55	2639.81

S6. Autocatalytic characteristics analysis

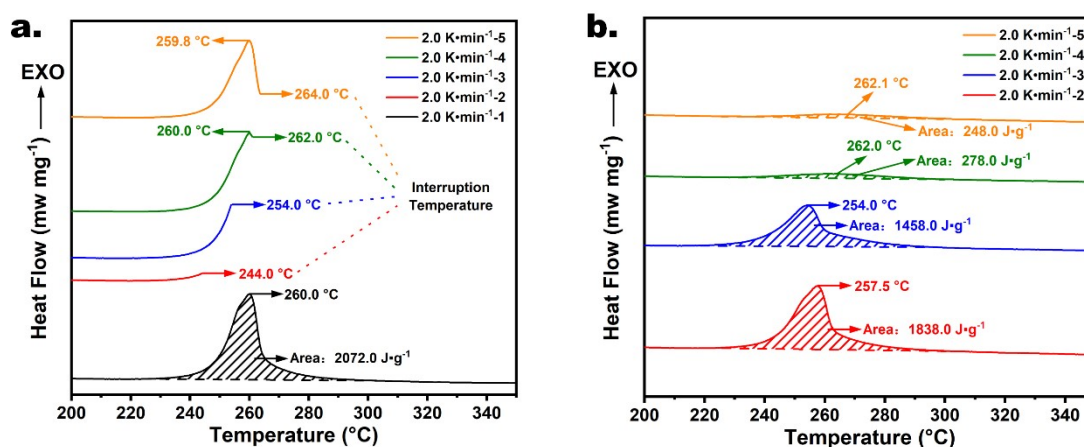**Fig.S3.** Comparison of the reheat curve (b.) at different interruption temperatures and the original curve (a) at the heating rate of 2.0 K•min^{-1}.

The thermal history experiments conducted at various interruption temperatures were illustrated in **Fig.S3**, while the experimental conditions and results are presented in **TableS5**. The BTA contained within an aluminum crucible with a pinhole was subjected to heating at four distinct interruption temperatures: namely, 244 °C, 254 °C, 262 °C, and 264 °C. This approach aimed to simulate different levels of thermal history experienced by the sample. The T_{peak} in the 2.0 K•min^{-1}-1 curve under the initial non-thermal history state was determined to be 260.0 °C, as evidenced by **Fig.5a** and **TableS5**. The corresponding conversion degrees α were found to be 0.03 and 0.24 at interruption temperatures of 244.0 °C and 254.0 °C, respectively, indicating the progress of the reaction. Subsequently, after undergoing thermal history, both T_{peak} values in the 2.0 K•min^{-1}-2 and 2.0 K•min^{-1}-3 curves shifted towards lower temperatures, as shown in **Fig.S3b**, resulting in a decrease in safety.

Therefore, the initial stage decomposition reaction of BTA can be characterized as an autocatalytic process. During storage and application, a gradual decomposition of stored BTA occurred, resulting in the formation of catalytic byproducts that facilitate its thermal degradation and effectively lower the onset temperature for decomposition. Consequently, it is imperative to

avoid extensive storage and heat sources to prevent any potential thermal history and further mitigate the risk of BTA explosion. After the thermal history, T_{peak} of 2.0 K•min^{-1}-4 and 2.0 K•min^{-1}-5 remained the same or increased slightly. Therefore, the second stage decomposition reaction of BTA was an n-order reaction.

TableS5. Thermal history experiment curves of BTA at different interruption temperatures.

Mark	Interruption temp./(°C)	Conversion degree α	T_{peak} / (°C)	$\triangle H$ / (J•g^{-1})
2.0 K•min^{-1}-1	-	-	260.0	2072.0
2.0 K•min^{-1}-2	244.0	0.03	257.5	1838.0
2.0 K•min^{-1}-3	254.0	0.24	254.0	1458.0
2.0 K•min^{-1}-4	262.0	0.63	262.0	278.4
2.0 K•min^{-1}-5	264.0	0.67	262.1	247.7

S7. Kinetics model analysis---the thermal decomposition process of BTA•H$_2$O

Table S6. The relative contributions of three reaction processes to the overall reaction for BTA•H$_2$O pyrolysis.

β (°C•min^{-1})	Process 1 Relative contribution (%)		Process 2 Relative contribution (%)		Process 3 Relative contribution (%)	
	Region (°C)	%	Region (°C)	%	Region (°C)	%
1	114.40~146.13	8.9	209.26~368.46	53.5	368.46~624.60	29.8
2	115.73~152.53	9.8	209.20~368.13	51.5	369.20~691.33	33.0
5	118.16~174.16	10.2	209.16~368.16	49.0	368.82~690.82	36.6
10	120.65~177.48	9.4	208.81~368.48	47.6	369.15~691.15	37.4
Average		9.6		50.4		34.2

TableS7. Kinetic model test for BTA•H$_2$O pyrolysis in first stage.

Method/Kinetic Model			R^2	S^2	MR	F-Test
Method: Friedman			0.99814	143.459	0.281	3.057
Kinetic Model	A→B	B→C				
A→B→C	A$_2$	F$_1$	0.99919	62.599	0.175	1.061
	A$_3$	F$_1$	0.99875	96.560	0.235	1.637
	A$_3$	F$_n$	0.99880	92.809	0.232	1.575
	A$_n$	F$_n$	0.99924	58.851	0.172	1.000

TableS8. Kinetic model test for BTA•H$_2$O pyrolysis in second stage.

Method/Kinetic Model			R^2	S^2	MR	F-Test
Method: Friedman			0.99937	1148.864	0.456	1.101
Kinetic Model	C→D	D→E				
C→D→E	C$_1$	F$_n$	0.99922	1419.811	0.553	1.240
	C$_n$	F$_n$	0.99933	1221.060	0.463	1.067
	C$_{n,m}$	F$_n$	0.99935	1185.166	0.448	1.036
	KS	F$_n$	0.99938	1143.223	0.426	1.000

TableS9. Kinetic model test for BTA•H$_2$O pyrolysis in third stage.

| Method/Kinetic Model			R^2	S^2	MR	F-Test
Method: Friedman			0.99872	827.545	0.488	1.136
Kinetic Model	E→F	F→G or G→H				
E→F	F$_n$	-	0.99800	1290.855	0.686	1.575
E→F→G	F$_n$	C$_1$	0.99822	1149.265	0.658	1.405
	F$_n$	C$_n$	0.99869	846.576	0.581	1.036
	F$_n$	C$_{n,m}$	0.99873	816.948	0.567	1.000
	F$_n$	KS	0.99866	866.348	0.578	1.061
E→F G→H	F$_n$	C$_n$	0.99860	902.506	0.593	1.104
	F$_n$	C$_{n,m}$	0.99860	901.475	0.591	1.103
	F$_n$	KS	0.99849	975.250	0.630	1.194

S8. Thermal decomposition mechanism analysis
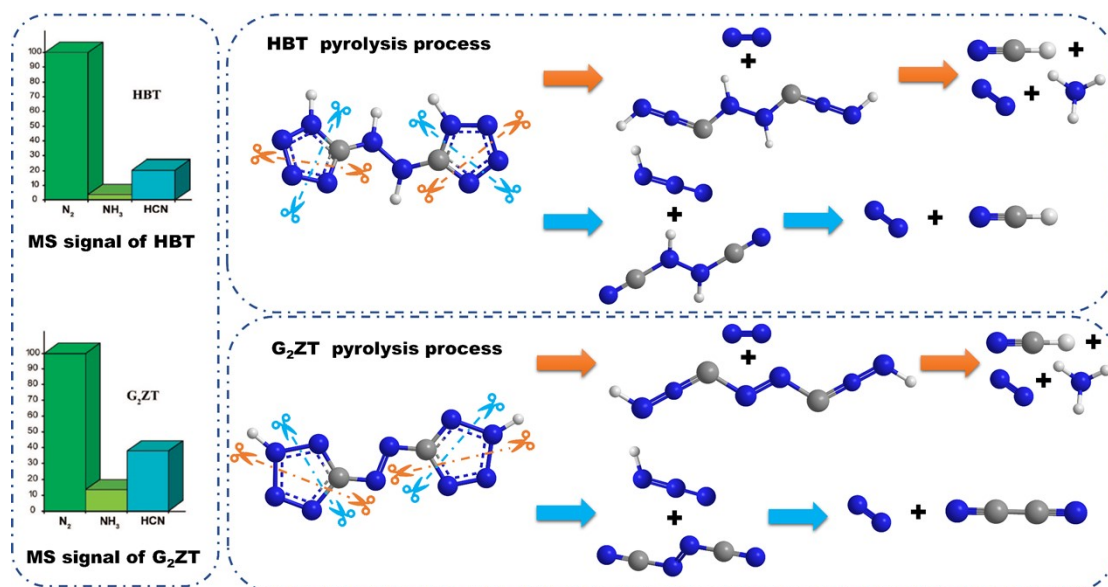
Fig.S4 The pyrolysis products of HBT and G_2ZT.